Influence of Anatomy, Microstructure, and Composition of Natural Fibers on the Performance of Thermal Insulation Panels

Melek Ayadi, César Segovia, Ayda Baffoun, Riadh Zouari, Vanessa Fierro, Alain Celzard, Slah Msahli, Nicolas Brosse

ACS OMEGA

Open Access

http://pubs.acs.org/journal/acsodf

Article

Influence of Anatomy, Microstructure, and Composition of Natural Fibers on the Performance of Thermal Insulation Panels

Melek Ayadi, César Segovia, Ayda Baffoun, Riadh Zouari, Vanessa Fierro, Alain Celzard, Slah Msahli, and Nicolas Brosse*

Cite This: *ACS Omega* 2023, 8, 48673−48688

Read Online

ACCESS | Metrics & More | Article Recommendations | Supporting Information

ABSTRACT: The growing interest in environmentally friendly materials is leading to a re-evaluation of natural fibers for industrial applications in order to meet sustainability and low-cost objectives, especially for thermal insulation of buildings. This paper deals with the chemical and physical characterization of fibers extracted from seagrass (*Posidonia oceanica*) and alfa grass (*Stipa tenacissima*) for a possible substitution of synthetic materials for thermal insulation. Hemp (*Cannabis sativa*), a fiber broadly used, was also studied for comparison. The parameters characterized include porosity, thermal degradation, elemental composition, skeletal and particle density of the fibers as well as investigation of the thermal conductivity of fiber-based panels. Several technologies were involved in investigating these parameters, including mercury intrusion, thermogravimetric analysis, fluorescence spectroscopy, and fluid pycnometry. The fibers showed a degradation temperature between 316 and 340 °C for *Posidonia*, between 292 and 326 °C for alfa, and between 300 and 336 °C for hemp fibers. A high porosity allied with a reduced pore size was revealed for *Posidonia* (77%, 0.54 μm) compared to hemp (75%, 0.61 μm) and alfa (57%, 2.1 μm) raw fibers, leading to lower thermal conductivity values for the nonwoven panels based on *Posidonia* (0.0356−0.0392 W/m.K) compared to alfa (0.0365−0.0397 W/m.K) and hemp (0.0387−0.0427 W/m.K). Bulk density, operating temperature, and humidity conditions have been shown to be determining factors for the thermal performance of the panels.

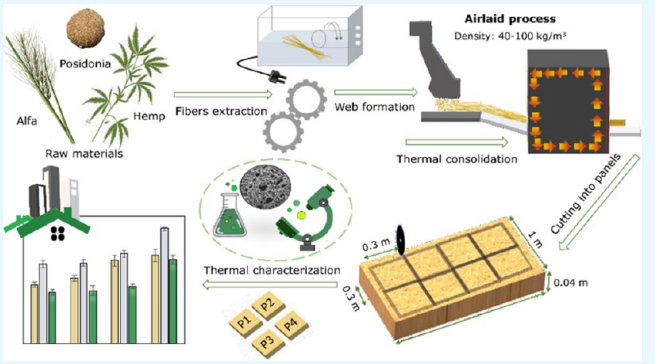

INTRODUCTION

In the global context of reducing the use of synthetic materials from petrochemicals, sustainable resources appear to be one of the major challenges facing industrial players. The European Commission in 2017[1] reported that synthetic fibers represent about 75% of the total fiber market in Europe coupled with various decisive factors related to the well-prospering chemical sector, increased production in textile materials, imminent specifications in the construction field, as well as considerable growth in the automotive and aerospace industry. Statistical analysis showed that combustion of fossil fuels is the main source of CO_2 emissions. In 2020, global CO_2 emissions from fossil fuels were around 34.8 $GtCO_2$.[2] A considerable part of these emissions is attributed to "nonenergy" applications, i.e., about 11−12% of the total amount of fossil fuels for final consumption in the 15 countries of the European Union (EU-15, values for 1995/1996).[3] This includes, for instance, the energy used for the manufacturing and processing of synthetic materials, which has a negative impact on the climate situation.[4] For these reasons, effective strategies are constantly emerging with the aim of replacing synthetic products with biosourced fibers and derivatives due to their attractive characteristics, including availability, biodegradability, low cost,[5] minimal health risks to workers during manufacturing and transportation of final products to sites, reduced energy requirements, as well as competitive technical performance in terms of being lightweight and possessing high porosity and thermal and acoustical efficiency.[6] As a result, biosourced fibers such as hemp, jute, sisal, cork, kenaf, and flax are increasingly used in various applications including packaging materials, biomedical composites, automotive nonwovens and textiles (roof, rear wall, side panel lining), thermal and acoustic insulation of buildings, etc.[7] Consequently, characterization remains the key parameter to establish the necessary data for the optimal use of available natural fibers. Fibrous waste derived from marine algae waste such as *Posidonia oceanica* seagrass is a source of fibers that has not yet been fully exploited.[8,9] *Posidonia* is a flowering marine plant that is endemic to the Mediterranean Sea, covering a quasi-

Received: May 22, 2023
Accepted: September 7, 2023
Published: December 13, 2023

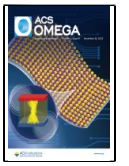

continuous area of the Mediterranean coasts (between 30 000 and 40 000 km^2) locally interrupted at estuaries and ports.[10] The dead leaves, most often lost in autumn, are transported by storms and can thus be found along sandy coasts. These fibers, in the form of balls of a few centimeters thick, are called sea balls ("Aegagropila" or "Pillae marinae").[11] Although they play an ecological role in protecting coasts from erosion, these leashes have a negative impact on tourism and are therefore frequently removed from beaches. When solid waste decomposes in landfills, it creates landfill gases, which are primarily composed of CO_2 and CH_4. There are several well-established, low-cost methods to reduce greenhouse gases from consumer waste, including recycling programs, waste reduction programs, and landfill methane capture programs.[12] As a result, the valorization of this renewable and inexpensive biomass for producing more environmentally friendly industrial products is both an economic and an ecological challenge. In recent years, research has been conducted to explore the use of *P. oceanica* as a polymer matrix reinforcement to develop natural composites, based on a mixture of *P. oceanica* and pine wood particles in a polyurethane matrix, and investigate their performance as structural panels.[13] Other authors evaluated the minimum bulk density for the use of *Posidonia* as a building solution on a flat roof.[14]

Stipa tenacissima is a perennial grass of arid and semiarid lands of North Africa and southern Spain. Its Arabic name is the alfa plant. The alfa plant is mainly present in Algeria and Morocco, representing about 4 and 2.2 million hectares of natural steppes, respectively.[15,16] In Tunisia, the alfa plant is mainly present in the region of Kasserine and covers about 12 000 000 ha.[17] Currently, alfa fibers are mainly used in high-quality paper and handicraft industries as well as in decoration and thermoplastic products.[18] Studies have investigated the mechanical behavior of alfa fibers embedded in a cement matrix[19] or the possibility of using the alfa fiber as a reinforcement for polymer composites.[20,21] Its major limitation is the difficulty in separating the fibers, which usually requires the coupling of chemical, enzymatic, and mechanical processes.[22] Hemp is a bast fiber extracted from plants growing up to 1.2−4.5 m, mainly cultivated in Europe, North America, and Asia. The global production volume of hemp fibers is estimated to be about 174 027 tons in 2020.[23] It is used in a variety of industries, including home textiles, composites, building insulation materials, and animal bedding.[24]

In 2021, nonwoven production in Europe increased in volume by 2.0% to reach 3 120 967 tonnes, with a significant growth recorded for the building construction sector (+17.4%).[25] Nonwoven fabrics are defined as sheet or web bonded by entangling fibers or filaments, mechanically, thermally, or chemically. Several development and consolidation methods can be considered,[26] leading to a variety of nonwoven products with different properties. Among them, Airlaid technology consists of forming a web by mixing fibers with air to form a uniform air−fiber mixture, which is then projected on a moving air-permeable belt or wire. Fibers of various lengths (1−100 mm) can be used, and cohesion is ensured by a moderate quantity of thermoplastic resins (∼10% wt).

In this paper, the physicochemical characteristics of both *P. oceanica* and *S. tenacissima* were established in comparison with hemp fibers by investigating their microstructure, chemical and elemental composition, density, porosity, as well as thermal stability. The production and thermal characterization of insulating panels based on fibers manufactured by the airlaid nonwoven technology were also presented. The effect of density, operating temperature as well as humidity conditions on the thermal conductivity of the panels was investigated.

MATERIALS AND METHODS

Fiber Extraction and Panel Processing. *Posidonia* fibers were manually extracted from *P. oceanica* balls and used in this study. They were collected on the coasts of Bizerte, northern Tunisia, in mid-March, when the ambient temperature was around 16 °C. The fibers were then sun-dried for 48 h. The balls are usually removed from the beaches by municipalities before the summer periods, and the residual material is disposed of in landfills. The fibers were used without further processing. The alfa plants used in this work were collected in the governorate of Kasserine. Extraction of the alfa fibers was carried out in NaOH (2.5 N) at 80 °C for 3 h and then being washed with distilled water and acetic acid to neutralize excess NaOH. The chemical treatment was followed by mechanical extraction of the dried fibers in a fiber opening machine to properly separate the elementary fibers and better evaluate their morphological properties. Three types of nonwoven panels (Figure 1) were developed in this work using airlaid technology, consisting of *P. oceanica*, alfa, and hemp fibers mixed with 10 wt % (PE)/(PET core) bicomponent short fibers (6 mm). A thickness of 40 mm was obtained by thermocompression at 170 °C of several plates of the initial material and then measured under the same experimental conditions.

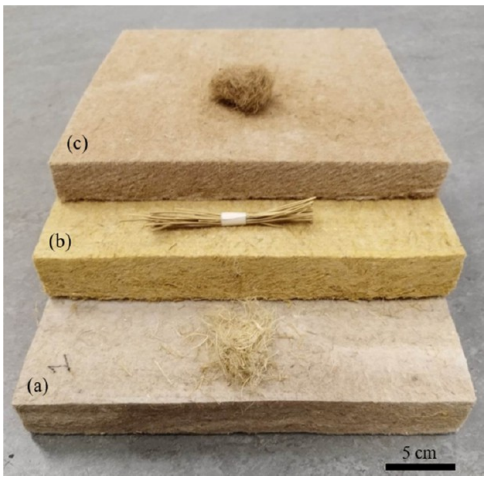

Figure 1. Nonwoven panels of 30 × 30 cm^2 prepared by airlaid technology: (a) Hemp, (b) Alfa, and (c) *Posidonia*. (*Note to Annual Reviews: Figure 1 is an original figure created by one of the authors for this article; it is not based on any previously published image*).

Morphological Analysis. The morphological examination of the fibers was performed using a Hitachi TM3000 scanning electron microscopy (SEM). This technique was applied to observe the surface morphology of the fibers. Prior to observation, the fibers were manually separated, parallelized, and metalized. They were then introduced into the sample holder via SEM. The images were taken at an acceleration voltage of 15 kV.

Chemical Composition. The chemical composition (cellulose, hemicelluloses, and lignin) of the *Posidonia*, hemp,

https://doi.org/10.1021/acsomega.3c02481
ACS Omega 2023, 8, 48673−48688

and alfa samples was quantified by the Van Soest method.[27] The tests were carried out on 1 g of material with three replicates for each sample, using a raw fiber extractor device manufactured by FOSS. This method allows determination of the biochemical content by fractionation of the plant material using different solvents. The results of the different chemical parameters were expressed on a dry basis. The analytical dry matter was measured in a ventilated oven at 105 °C for 48 h. Cellulose, hemicelluloses, and lignin were determined from the neutral detergent insoluble residue (NDF), acid detergent insoluble residue (ADF), and acid detergent and H_2SO_4 (%) (w/w) insoluble residue.

Ash Content. Cultivation site, local climatic conditions, season, and harvesting mode are determinant factors influencing the elemental composition and structure of natural fibers.[28] The ash content of *Posidonia*, alfa, and hemp samples, expressed as a percentage of the initial dry weight, was determined by weighing the residue remaining after combustion in a muffle furnace at 600 °C for 12 h until all carbon was eliminated. The ash content in the raw material was calculated using eq 1

$$\text{total ashes}(\%) = \frac{\text{weight of the residue after ashing (g)}}{\text{weight of raw dry, material (g)}} \times 100 \quad (1)$$

Elemental Analysis. XRF is a nondestructive, quantitative, and widely available technique for elemental analysis of a material.[29] When highly focused X-rays or energetic electron beams irradiate a material, an X-ray photon transfers its energy to an electron in the inner shell of an atom of the material. In the case where the energy of this photon is higher than the binding energy of the electron, the latter is ejected from its atomic orbital, and thus, an electron from an outer shell falls to fill the empty position of the ejected electron, emitting a photon of energy equal to the difference between the electronic energy levels involved. Since this energy difference depends strictly on the electronic layers of a given atom, the re-emitted X-ray photon—hence the name fluorescence—is characteristic of the element encountered, which therefore allows it to be identified and quantified.[30] In this study, XRF was performed to provide information on the elemental composition of *Posidonia*, hemp, and alfa fibers. Measurements were performed on disk-shaped samples by wavelength-dispersive XRF, using a QANT'X EDXRF ARLAnalyser operated at an X-ray beam excitation voltage of 7 kV. The samples were previously dried and pressed into a disk form for measurements.

Microstructure and Density Characterization Methods. *Bulk Density Measurement.* The bulk density was determined by the tap density method on raw and ground fibers to evaluate the effect of the grinding process on the microstructure of the samples. An automatic procedure was used to measure this density using a QUANTACHROME AT-6 AutoTap density meter. The samples were dried at 70 °C for 24 h and then introduced into a graduated glass test tube and carefully leveled without compaction. The container was then mechanically tapped on the rigid surface of the AutoTap device a given number of times. In this way, the fibers are progressively compacted to a constant density value. This technique measures the random packing density of the sample and gives an indication of how the particles flow. The packing properties of fibers or a powder can affect operations related to solid dosing, including bulk storage, fiber/powder flow, and compaction.

True Density Measurement. Pycnometry is a technique for measuring the absolute volume of solid materials using Archimedes' principle of fluid displacement and Boyle's law of gas expansion. The sample is introduced into a cell of a determined and very precise volume, and the quantity of fluid that can be placed in it is measured. The test is performed at room temperature and atmospheric pressure. The volume of the solid skeleton of the sample can be determined according to the ability of the gas to penetrate the porosity of the sample. Knowing the mass of the sample, the skeletal (true) density can be calculated. The fibers were dried at 70 °C for 24 h and kept in a desiccator until testing. They were then introduced into the sample holder of an Accupyc 1340 Helium Pycnometer (MICROMETRICS). Helium was used as the displacement gas. As helium is a light gas and as its molecules are small enough to penetrate pores larger than 0.2 nm, helium pycnometry can appropriately provide the true density of the material in the case where the sample does not have sealed pores.[31] Nevertheless, significant errors can occur when the sample is likely to release volatile components into the helium atmosphere, such as during the possible dehydration of materials in the measurement process.

Sample volume measurements are made by filling the sample holder with helium to a given target pressure. Then, the gas is expanded in a reference volume by opening the valve that connects it to the sample holder. The final pressure at equilibrium (P_f) that is reached is then measured. The volume of the sample is calculated by measuring the change in fluid pressure provided by the displacement by the sample of helium at constant volume, according to the following equation based on the gas law with the assumption of a constant total number of gas molecules in a closed system (eq 2)

$$V_{\text{sample}} = V_{\text{sampleholder}} + V_{\text{reference}} \frac{P_f - P_2}{P_f - P_1} \quad (2)$$

where V_{sample}, $V_{\text{sample holder}}$, and $V_{\text{reference}}$ are the volumes of the sample, sample holder, and reference cell, respectively, and P_f, P_1, and P_2 are the final pressures after expansion of helium from the sample holder to the reference cell, the filling pressure in the sample holder, and the pressure in the reference cell before opening the valve, respectively.

In this test, the number of successive measurements was set to 12. The cell volume was 11.1850 cm, and the reference volume was 9.1825 cm^3. An equilibrium rate of 0.005 psig/min was used at 23 ± 1 °C. The results are presented as density values and standard deviations corresponding to five replicates for each sample. Note that the true density of the samples can also be measured by mercury intrusion (see the next section), provided that all narrow pores are accessible to mercury at the maximum pressure used and that the sample does not collapse under pressure. On the other hand, the apparent (or envelope) density is calculated with the measured volume and the known weight of the sample.

Envelope Density Measurement. The envelope density is defined as the mass of a material divided by its volume including that of its pores and small cavities. The envelope density of raw and ground fibers was measured by using a GeoPyc 1360 system. The diameter of the internal chamber used was 12.7 mm, and the force applied was 5 N. The results represent the average values obtained over 12 measurement cycles for each sample.

https://doi.org/10.1021/acsomega.3c02481
ACS Omega 2023, 8, 48673−48688

Porosity. *Fiber Porosity.* Mercury intrusion porosimetry (MIP) is a technique for studying porosity in terms of both measuring pore volumes and evaluating pore size distributions. It allows characterizing pores from a few nanometers to a hundred micrometers in diameter. As a nonwetting medium, mercury must be forced to penetrate into the Hg-accessible open porosity of a porous solid by increasing its pressure. In the low-pressure stage, mercury fills the contours of the sample. Its apparent volume can therefore be deduced, and thus, its apparent density can be calculated. Nevertheless, it is not possible to ensure that mercury has not been introduced into the very large pores during this stage. Conversely, at high pressure, and assuming that no smaller porosity remains that can be reached with increasing pressure, it is supposed that mercury penetrates all accessible porosities in the material and the skeletal density can be deduced. The pore volume can be determined from the amount of mercury intruded. The calculation of the pore size distribution requires knowledge of the relationship between the imposed pressure P and the diameter D of the intruded pores given by the Washburn eq 3, the pores being supposed to be cylindrical and gradually intruded from the largest to the narrowest as the pressure increases

$$D = \frac{-4\gamma\cos\alpha}{P} \tag{3}$$

where γ is the surface tension of mercury (0.48 N/m) and α is the contact angle of mercury with the material (141°).[32] One drawback of this technique is the risk of crushing the sample by increasing the pressure during the analysis process. In addition, the MIP method can have a limitation in differentiating interparticle from intraparticle porosity, especially for powders. Moreover, this technique estimates only the pore throat diameter, different from the actual pore size for bottle-shaped pores. Yet, the Washburn equation has been generally accepted as a practical method for analyzing complex systems whose pores are rarely cylindrical.[33] Furthermore, the total porosity provided by this technique can be considered reasonable because, by the time the high pressure is reached, either all of the pores will have been intruded or the pore walls will have been crushed and their equivalent volume effectively intruded. In this work, MIP was carried out with an Autopore IV Porosimetry (Micrometrics) instrument to measure macro- and mesopores from 360 to 3.6 μm for low-pressure analysis and from 6 to 0.003 μm for high-pressure measurements. Prior to any measurement, the samples were dried at 70 °C in an oven and then introduced into the penetrometer. The particles were introduced manually, and the penetrometer was slightly agitated to allow for the densest possible stacking, enabling the maximum number of particles to be introduced. The results were reported in a graphical form. In a first graph, the cumulative pore volume was plotted as a function of intrusion pressure, and in the second, the pore size distribution was calculated via eq 3 and plotted in the logarithmic form $dv/d\log R$.

Panel Porosity. The open porosity measurement[34] is used to determine the air volume within a sample of a porous material based on the mass measurement of the material saturated by a heavy fluid at different pressures. The open porosity of air-saturated open-cell porous panels was measured at a density of 90 kg/m^3 on three samples for each material. The open porosity and bulk density of the skeleton are deduced from the measurement of four masses and four static pressures. The mass of the chamber in which the sample is introduced is measured under vacuum, giving the value M_1, and under argon at a pressure of 8 bar, giving the value M_2. Then, the same measurements are made with the sample: under vacuum, leading to M_3, and under pressure, leading to M_4. Assuming that the gas used behaves as a perfect gas under the operating conditions, using the law of perfect gases in isothermal compression, the porosity is deduced as described in eq 4

$$\Phi = 1 - \frac{RT}{V_t}\left(\frac{M_2 - M_1}{P_2 - P_1} - \frac{M_4 - M_3}{P_4 - P_3}\right) \tag{4}$$

where R is the specific gas constant, T is the temperature in Kelvin, V_t is the volume of the tested materials, and P_i (i = 1, 2, 3, 4) are the measured pressures. The porosity measurements were performed on samples of a thickness of 40 mm and a density of 90 kg/m^3.

Thermogravimetric Analysis Thermogravimetric Analysis (TGA). The thermal stability of the fibers was evaluated by thermogravimetric analysis (TGA) on a NETZSCH STA 449F3 ST instrument. The temperature was raised from 28 to 900 °C at a heating rate of 10 °C/min under an argon atmosphere. The last 30 min was performed under an air atmosphere to estimate the ash content.

Calorimetric Analysis. Calorimetric experiments were performed using a Parr 6200 calorimeter. The fibrous pellets were prepared using a Specac GS 15011 manual hydraulic press, and the samples were then sealed in a steel crucible for examination. All experiments were performed under an air atmosphere at 30 bar from 20 to 500 °C at a heating rate of 10 °C/min.

Thermal Conductivity Measurements. The steady-state thermal conductivity for the three types of panels was determined on 300 × 300 mm^2 specimens using a hot/cold plate apparatus according to NF EN 12667. The flowmeter method is based on the application of Fourier's law, generating a unidirectional heat flux across both surfaces of the sample. The thermal conductivity is then determined by measuring the steady-state heat flux and the temperature difference between the hot and cold sides of the samples. Thermal conductivity is first measured at respective cold and hot plate temperatures of 0 and 20 °C to ensure an average temperature of 10 °C and then at 10 and 30 °C to obtain an average temperature of 20 °C. In order to investigate the influence of the humidity content on the thermal performance of the panels, thermal conductivity was performed on samples dried in an oven at 70 °C to a relative humidity close to 0% as well as panels preconditioned under 23 °C and 50% RH until almost no mass change. The thermal conductivity (k) in one dimension can be described by the simplified form of Fourier's law (eq 5)

$$q = -kA(dT/dx) \tag{5}$$

where q is the steady-state heat flux in the x-direction (w/m^{-2}), A is the cross-sectional area of the sample (m^2), and $-dT/dx$ is the temperature gradient (K/m). The sample with a thickness of 40 mm and a cross-sectional area of 300 × 300 mm^2 was sandwiched between the two flowmeter plates. The hot plate acted as both a temperature sensor and a heat source. The thermal conductivity was then determined from the heat flux and temperature difference across the thickness of the sample.

https://doi.org/10.1021/acsomega.3c02481
ACS Omega 2023, 8, 48673−48688

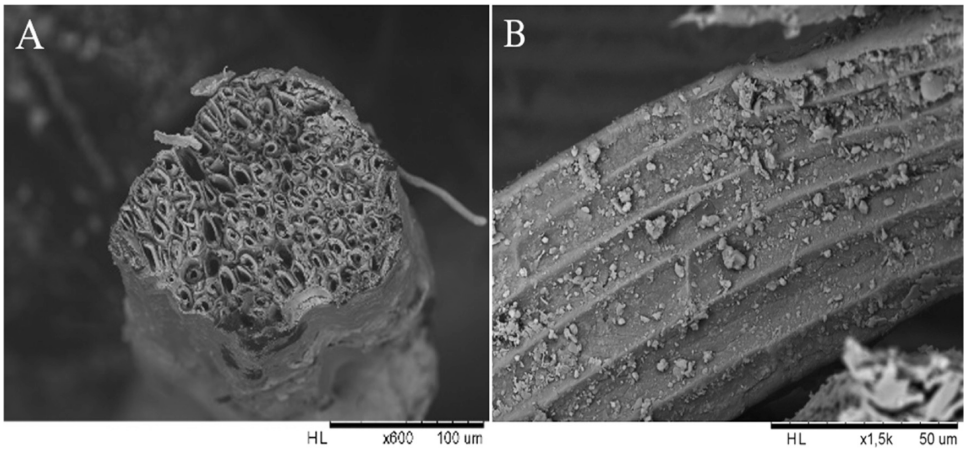

Figure 2. Scanning electron microscopy (SEM) micrographs of *Posidonia* fibers. Scale bar is equal to (A) transversal cross section 100 μm and (B) longitudinal cross section 50 μm.

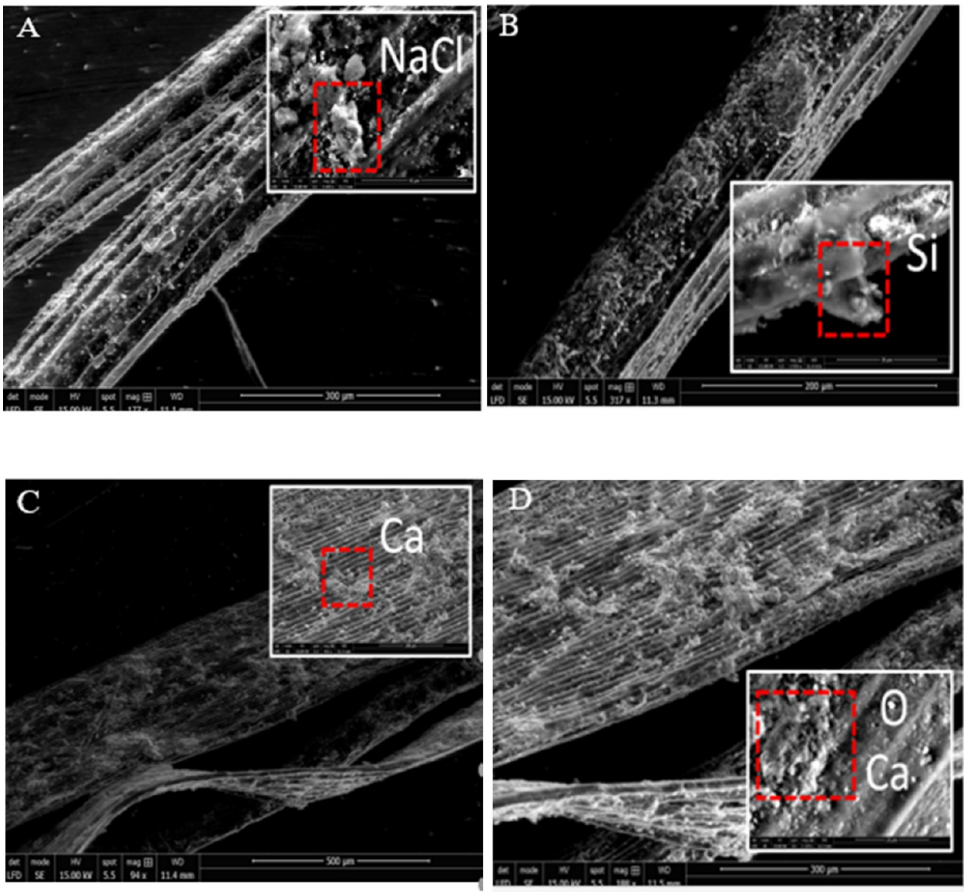

Figure 3. Scanning electron microscopy (SEM-EDS) micrographs of *Posidonia* fibers. Scale bar is equal to (A) 500, (B) 300, (C) 200, and (D) 20 μm.

Tension Strength. Tensile strength was evaluated according to NF EN 1607. The aim of this test was to determine the resistance to tension perpendicular to the surface of the specimen by submitting it to a uniformly distributed tensile force until rupture occurs. For this experiment, three samples were tested for each material. Square specimens with a side length of 200 ± 3 mm and a density of 65 ± 3 kg/m^3 were tested. Prior to the test, wooden blocks compatible with the fixing device were glued to specimens by using PVA glue. The specimens with glue on blocks were preconditioned at 23 °C and 50% RH for 24 h and then put under a load. In this test, a Galdabini Quasar 25 testing machine was used. The test was performed at a tensile speed of 10 mm/min, where the maximum load sustained by the test piece with a precision of 1% was recorded.

RESULTS AND DISCUSSION

Morphology. The morphological characterization of *Posidonia*, alfa, and hemp fibers was carried out using the SEM technique. It is clear from Figure 2 that the raw *Posidonia*

https://doi.org/10.1021/acsomega.3c02481
ACS Omega 2023, 8, 48673−48688

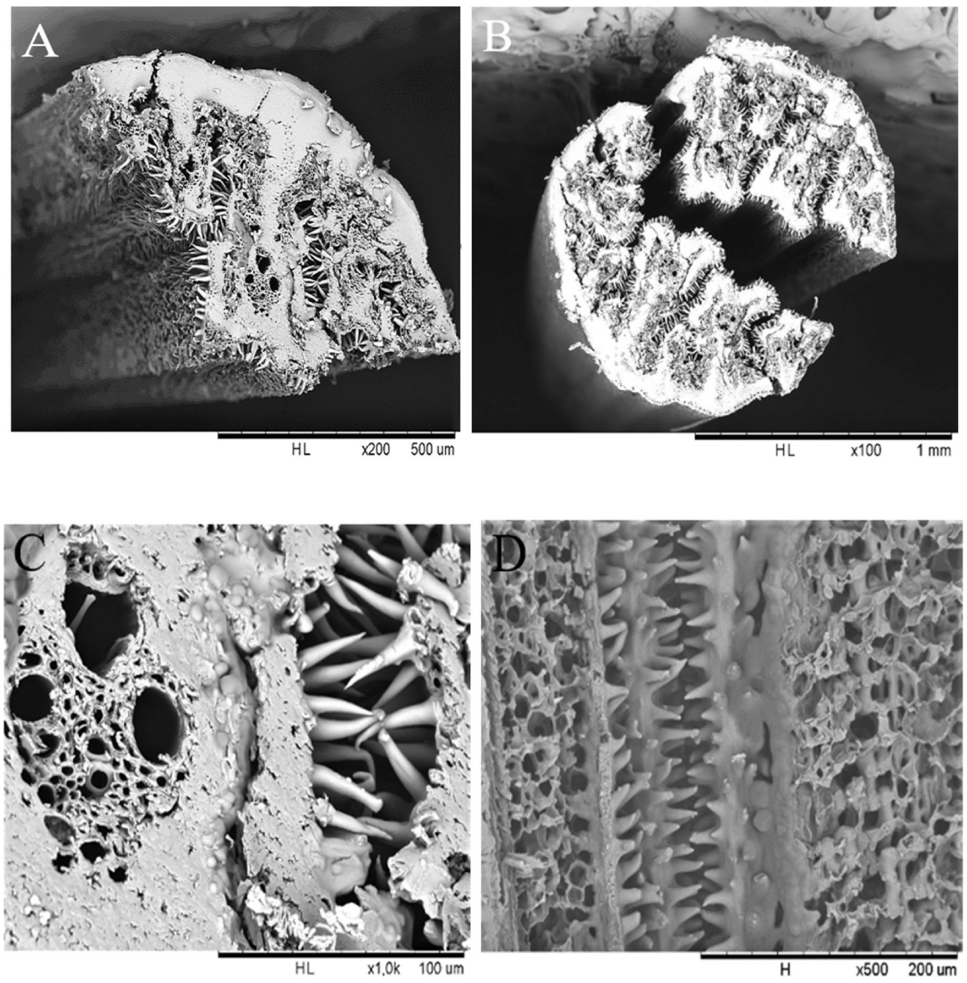

Figure 4. Scanning electron microscopy (SEM) micrographs of alfa fibers. Scale bar is equal to transversal cross section (A) 500 μm, (B) 1 mm, (C) 100 μm; and longitudinal cross section (D) 200 μm.

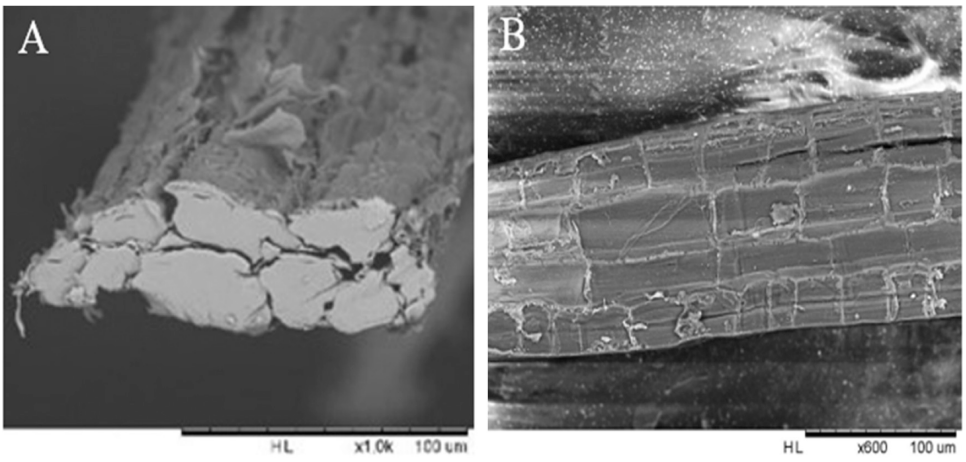

Figure 5. Scanning electron microscopy (SEM) micrographs of Hemp: (A) transversal cross section and (B) longitudinal cross section; scale bar is equal to 100 μm.

fiber with a cylindrical shape has a rough nonporous transversal surface and is composed of an assembly of fibrils consisting of several ultimate cells and fibers presenting small cavities (lumen). The average diameter of the *Posidonia* fibers was evaluated by analyzing SEM images using a digital image analysis (ImagePro Plus). From this analysis, an average diameter of 94.37 ± 4.72 μm for *P. oceanica* was measured on 25 fibers, confirming the micrometer scale of the fiber. The pore diameter range is approximately 0.2−25 μm. SEM-EDX micrographs of *Posidonia* fibers showed the presence of sodium, chlorine, and silicon (Figure 3A,B). The presence of calcium and oxygen (Figure 3C,D) was also noted, as well as that of different metallic and nonmetallic elements. With reference to available data, the elemental composition of

https://doi.org/10.1021/acsomega.3c02481
ACS Omega 2023, 8, 48673−48688

Posidonia fibers depends on different predominant factors including the season, the age of the plant, the site of origin as well as the level of anthropization.[35] Textural characterization of alfa fibers (Figure 4) showed a cavernous cylindrical structure composed of several filaments spanning the length of the plant. As an assembly of lignocellulosic filaments, the fibers have an absorbent character allowing the longitudinal opening or closing of the leaf according to the relative humidity conditions.[22] The pore size range of the alfa fiber is about 0.1−40 μm. The longitudinal view shows that the surface of the alfa fiber is covered with a dense hairy layer, allowing sufficient adhesion to form the plant stem. In accordance with previous reports,[36] SEM images of hemp (Figure 5) showed that the fiber is composed of an assembly of cells or ultimate fibers arranged in bundles presenting an average diameter of ∼48.7 μm (measured on 25 fibers with ImagePro+). The bundles are composed of several unitary fibers joined by pectin and other cementing compounds such as lignin and hemicellulose to constitute the technical fiber, confirming that the mechanical extraction consisting of the carding process was insufficient to properly divide all of the technical fibers into smaller individual fibers. Fiber length was 19.4 ± 13.5 mm for *Posidonia*, 41.7 ± 16.4 mm for alfa, and 46.6 ± 8.2 mm for hemp, measured on 100 extracted fibers.

Chemical Composition. The physical and chemical properties of plant fibers are considerably affected by their constituents. For example, the lignin content strongly influences their structural properties and morphology; the mineral components of the fibers affect their flammability; and the waxy substances influence their wettability and their adhesion properties. The chemical compositions of the three fibers are shown in Table 1. These results are obtained for

Table 1. Contents of Main Chemical Constituents of P. oceanica, Alfa, and Hemp Extracted Fibers

fibers	cellulose (%)	hemicelluloses (%)	lignins and cutin (%)	water−soluble compounds (%)
Posidonia	45.3 ± 2.1	19.7 ± 1.7	31.5 ± 0.9	3.6 ± 0.8
Alfa	47.4 ± 2.8	28.9 ± 0.9	10.7 ± 0.7	13.0 ± 0.9
Hemp	62.8 ± 2.9	19.3 ± 1.4	10.6 ± 0.6	7.3 ± 0.7

hemp mechanically extracted fibers, alfa fibers after chemical and mechanical extraction, and *Posidonia* manually separated raw fibers. As expected, holocellulose (cellulose + hemicelluloses) represents the major component of P*osidonia*, alfa, and hemp fibers with 65, 76.3, and 82.1%, respectively. These results are similar to those reported by Ncibi et al.[37] and Khiari et al.[38] for *Posidonia* fibers. It was also found that *Posidonia* fibers contain quite a high amount of lignin (∼31.5%) compared to the typical amounts found in nonwood plants,[39] hardwood,[40] and annual plants.[41] Although this amount of lignin is in the same range as that of softwood, it is higher than that of alfa and hemp fibers and some other natural fibers such as flax and kenaf.[42] This suggests the possibility of using these fibers to enhance fiber−matrix adhesion in composite materials. The cellulose content of *Posidonia* fibers (45.3%) is lower than that of hemp and alfa fibers but comparable to that of jute and kenaf fibers reported in another study.[43] These high contents could offer the possibility of using *Posidonia* fibers as cellulose derivatives for fiber-reinforced composite materials or the paper industry. Many authors studied the chemical composition of alfa fibers.[44,45] Mehdadi et al.[46] found that the chemical composition of the alfa plant could change depending on the harvesting season. For example, they found that leaves collected in spring had a relatively higher hemicellulose content compared with those collected in summer as a reaction of the plant to limit moisture loss during dry periods.

Ultimate Composition and Ash Content. The values obtained for elemental analysis and ash content for the different fibers are listed in Table 2. The results show that *P. oceanica* fibers present the highest ash content (9.84%) compared to alfa (5.38%) and hemp (1.84%) fibers. Khiari et al.[38] found 12% ash in *Posidonia* fibers collected in Monastir in August 2007. The differences may be related to climatic conditions, soil composition, etc. Thomsen et al.[47] found a value of 2−3 wt % measured on hemp fibers, while for alfa fibers, Akchiche et al.[48] found 4.6% ash content. Regarding the elemental composition of *Posidonia* fibers, the carbon, oxygen, and hydrogen contents were similar to those previously reported in other studies with *C* = 42−49% and *O* = 34−38%.[37,49] *Posidonia* residues were characterized by a very high content of chlorine (Cl) as well as calcium (Ca), silicon (Si), and sodium (Na) as confirmed by SEM-EDX analysis. This result is expected due to their marine origin, while hemp and alfa fibers were mainly characterized by the presence of potassium (K). The high sodium chloride content can explain the natural resistance to fungal growth of panels made of *Posidonia* fibers investigated in previous studies, as sodium chloride is known as an antifungal agent used routinely in the aquaculture industry.[50] These differences of ash content between the three fibers are related to their origin, as the mineral constituents of the environment where the natural fibers were grown strongly influence their elemental composition, depending on agronomic factors and the amount of soil contamination.[31]

Table 2. Elemental Analysis of *Posidonia*, Hemp, and Alfa Fibers

element	*Posidonia*	Alfa	Hemp
	(wt % on dry basis)		
ash	9.84	5.38	1.84
carbon	46.0	41.9	43.4
oxygen	42.9	47.2	50.3
nitrogen	0.17	0.03	0.43
hydrogen	5.5	6.1	6.2
sulfur	0.320	0	0.002
	(ppm)		
Cl	14 811	2037	2087
Si	8822	291	287
Ca	8723	3619	3868
Sx	4210	183	185
Fe	3148		
Al	3075		
I	1482		
K	993	6712	7050
Br	301		
Sr	129		
Co	42		

Absolute Density. The bulk densities of fibrous, powdery, and granular flaky materials depend on the way the particles are packed together due to cohesion and shape effects. All density results are shown in Table 3, from the packing scale

https://doi.org/10.1021/acsomega.3c02481
ACS Omega 2023, 8, 48673−48688

Table 3. Bulk, Particle, and Skeletal Densities of *P. oceanica*, Hemp, and Alfa Fibers (*F*) and Powders (*P*) at 23 ± 1°C

	bulk density ρ_B(kg/m^3)				particle density ρ_P (kg/m^3)		particle skeletal density ρ_S (kg/m^3)			
	GeoPyc		AutoTap		Hg		Hg		He	
	P	*F*	*P*	*F*	*P*	*F*	*P*	*F*	*P*	*F*
P. oceanica	553	100	532	34	503.3	289.3	1314	1238	1512.9	1528
Hemp	405	58	207	31	382.1	304.2	1246	1210	1537.0	1515
Alfa	418	70	82	31	349.1	541.2	1317	1268	15641	1544

Table 4. Porosity Characteristics of Fibers (*F*) and Ground Fibers (*P*) as Determined by Mercury Porosimetry in the Pressure Range of 0.0007−413.6854 MPa

fibers	nature (*F*/*P*)	sample weight (g)	skeletal density (g/cm^3)	total intrusion volume (cm^3/g)	total pore area (m^2/g)	median pore diameter (μm)	porosity (%)
Posidonia	*F*	0.17	1.24	2.65	2.12	0.54	76.6
	P	0.31	1.31	1.23	2.12	0.52	61.7
Hemp	*F*	0.19	1.21	2.46	0.58	0.61	74.8
	P	0.29	1.25	1.81	1.49	0.51	69.3
Alfa	*F*	0.11	1.27	1.06	0.33	2.10	57.3
	P	0.30	1.32	2.11	1.03	1.02	73.5

(ρ_B) to the particle skeleton scale (ρ_S). Comparing the two automatic methods for tapped density, it appears that densities obtained with the AutoTap device are systematically lower than those given by the GeoPyc apparatus. The Autotap method leads to values between 31 and 34 m/kg^3 for the raw fibers (*F*) and between 58 m/kg^3 and 100 m/kg^3 for the ground fibers (*P*), while the GeoPyc technique showed values ranging between 82 and 532 m/kg^3 for the fibers and between 405 and 553 m/kg^3 for the ground fibers. The main difference between the two methods was observed on alfa powders at a value of 418 m/kg^3 using the GeoPyc method and of 82 m/kg^3 using the AutoTap technique. The lower values of tapped density are due to interparticle voids and intraparticle porosity included in the volume measurement, while the Geopyc method only considers the envelope density of the particles. In this case, only the pore spaces inside the particles are included in the volume measurement.

The particle density evaluated by mercury intrusion was relatively close for hemp (382 kg/m^3) and alfa (349 kg/m^3) and lower than that of *Posidonia* powder (503 kg/m^3). It can be observed that the value obtained by Hg porosimetry is lower for *Posidonia* fibers (289 kg/m^3) compared to that obtained for the powder, which implies that part of the internal porosity of the fibers was not completely intruded by mercury in the low-pressure range but which the grinding into powder has made accessible.

The skeletal density of the fibers and the ground fibers was also analyzed using He pycnometry and Hg intrusion. It can be observed that, as expected, He pycnometry showed higher values for both fibers and powders. The literature provides a true density of 1500 kg/m^3 for hemp fibers and 1400 kg/m^3 for alfa fibers.[51] The absolute density of *Posidonia* fibers was 1.515 g/cm^3. This result is similar to that of flax fibers.[51] Due to their low density compared to synthetic materials such as glass fibers (2.4 g/cm^3), the tested fibers prove their potential application for the preparation of lightweight composites.

Porosity and Pore Size Distribution. Table 4 shows the total mercury intrusion volume, total porosity, and median pore diameter of *Posidonia*, alfa, and hemp fibers and powders measured by MIP. The total intrusion volume of *Posidonia* fibers is on average 2.65 cm^3/g, and the total pore surface area is around 2.1 m^2/g. The total accessible porosity of *Posidonia* fibers is about 77%, which is relatively higher than those of hemp (75%) and alfa fibers (57%). In the case of *Posidonia* and hemp, the accessible porosity of the ground fibers was lower than that measured on the original fibers. In fact, the porosity of the material depends on its particle size. For alfa fibers, the grinding process increased the open porosity of the grains from 57.3 to 73.5%.

The cumulative Hg intrusion curve is plotted as a function of pore size, and changes in the slope of the curve correspond to different ranges of pores (Figure 6). The extrusion curves are not shown but are horizontal, demonstrating that all of the intruded mercury remained trapped in the porosity of the samples, confirming the ink bottle-pore structure of the fibers. The two plateaus observed on the intrusion curves of the three fibers suggest that the pore size distributions are bimodal. The experimental results for *Posidonia* fibers show a first group of pores ranging from 0.06 to 6.03 μm (Figure 6a) and a second group ranging between 10.85 and 345.57 μm (Figure 6b). In addition, the pore size distribution measured by MIP shows a good agreement with the results of SEM (mentioned below). These pore sizes are higher than those observed on ground fibers, for which the two groups of pore sizes were in the ranges of 0.03−4.42 and 7.62−246.59 μm. Regarding mercury intrusion, hemp and alfa fibers also showed two separated peaks at 0.03−4.46 μm and 10.52−246.87 μm. The pore size distributions for alfa fibers are 0.20−6.03 and 9.65−275.63 μm. After grinding, no significant difference was observed on the ground materials, with pore diameters of 0.027−4.42 and 7.61−246.42 μm for ground hemp and 0.031−6.05 and 9.13−246.59 μm for ground alfa fibers. This result implies that while the grinding process increased the accessible porosity of the samples, it did not have a significant impact on the pore structure and therefore retained their initial structure.

Figure 7 shows a series of micrographs of the airlaid samples with the observable pores outlined in green, as obtained by ImagePro Plus analysis. This image analysis aims to represent the distribution of the fibers along the fiber web through the observable pores in the plane of the nonwovens. This in-plane porosity differs from the total open porosity of the nonwoven structure. All three nonwovens are highly porous and present quite similar open porosity values at a density of 90 kg/m^3. For the *Posidonia* sample, the in-plane porosity (12.19%) was lower

https://doi.org/10.1021/acsomega.3c02481
ACS Omega 2023, 8, 48673−48688

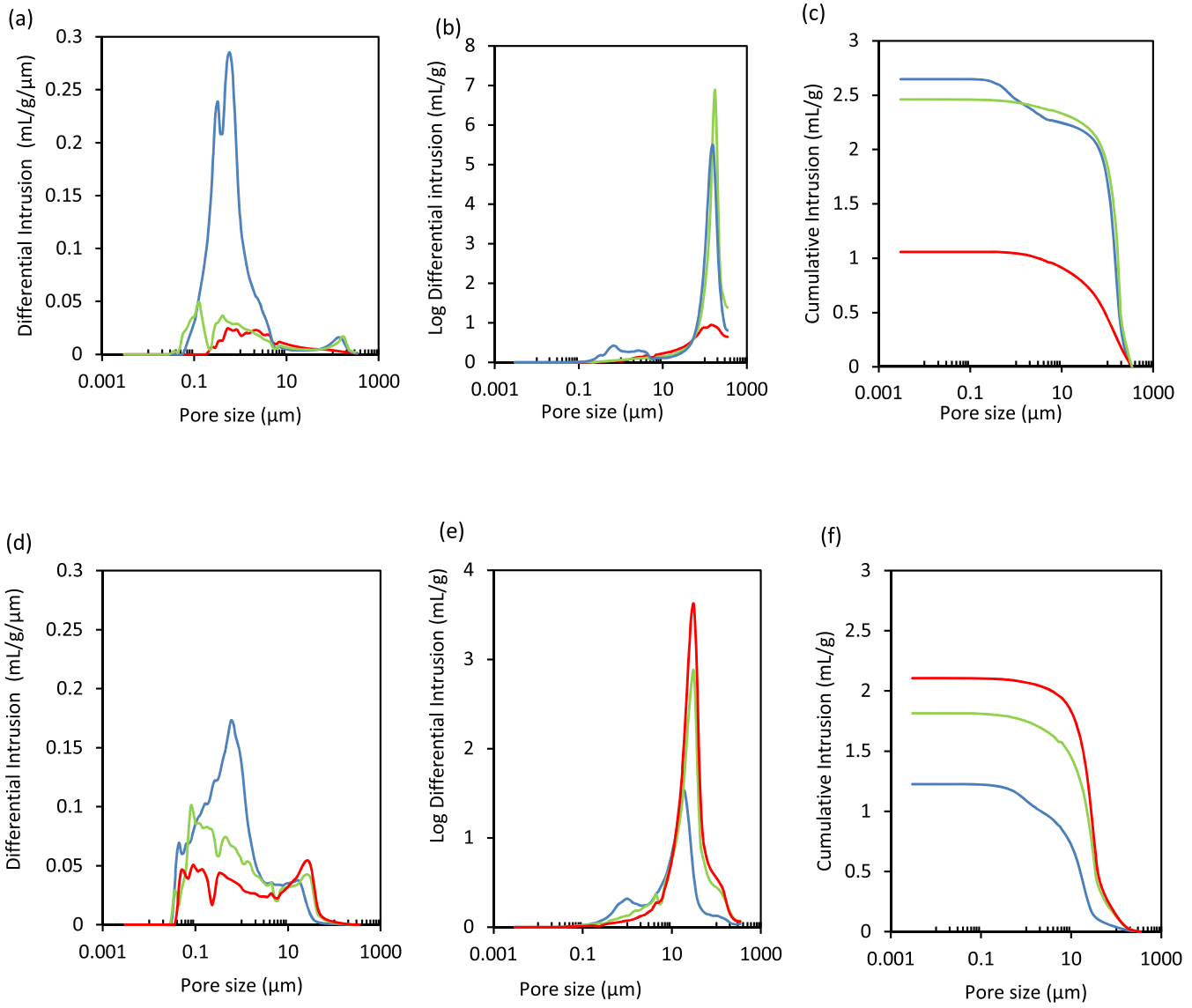

Figure 6. Mercury intrusion porosimetry: Differential intrusion (left), log differential intrusion (middle), and cumulative intrusion (right) as a function of pore size diameter for (a−c) fibers and (d−f) ground fibers. (blue straight line) *Posidonia*, (red straight line) Alfa, (green straight line) Hemp.

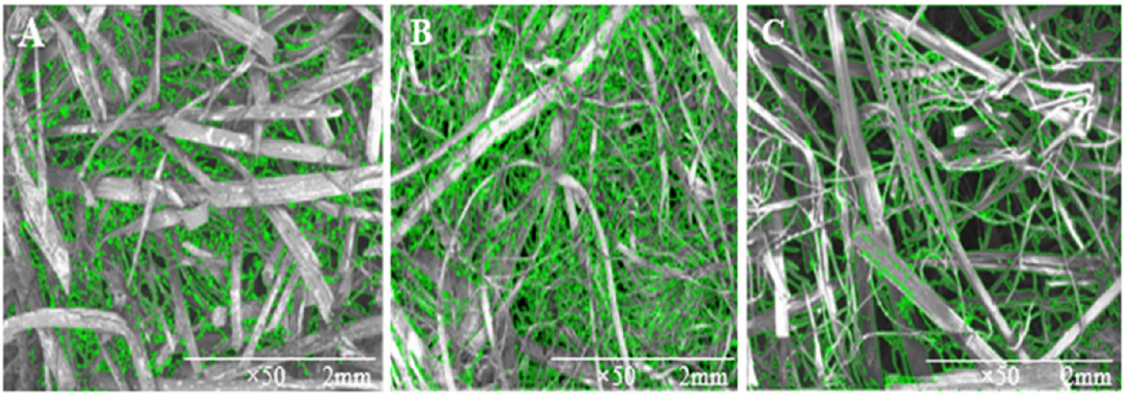

Figure 7. In-plane porosity of (A) *Posidonia*, (B) Alfa, and (C) Hemp airlaid samples by microscopy image analysis.

than for hemp (16.61%) and alfa (22.19%) (Table 5). This difference in in-plane porosity is attributed to the topology of the fibrous structure with more fiber-to-fiber interactions, with the *Posidonia* sample having shorter fiber lengths (19.4 ± 13.5 mm).

https://doi.org/10.1021/acsomega.3c02481
ACS Omega 2023, 8, 48673−48688

Table 5. In-Plane and Total Open Porosities of the Airlaid Panels

sample	in-plane porosity (%)	open porosity (%)
Posidonia	12.2	92.8 ± 0.004
Alfa	22.2	93.8 ± 0.005
Hemp	16.6	93.7 ± 0.006

TGA. Figure 8 shows the TGA/DTGA curves obtained for *Posidonia*, alfa, and hemp fibers. Table 6 reports the thermal analysis results obtained from these curves. As can be seen, all three samples showed two stages of weight loss in the temperature range 23−900 °C. The first stage takes place at a temperature range of about 45−145 °C, which is the result of the evaporation of structural moisture and volatile compounds. Thermal degradation of *Posidonia*, alfa, and hemp fibers occurred between 316 and 340, 292 and 326, and 300 and 336 °C, respectively. For hemp fibers, the main degradation event during the TGA experiments, under a nitrogen atmosphere, was between 220 and 450 °C, which is due to degradation processes of cellulose and hemicelluloses such as dehydration, decarboxylation, and depolymerization before the formation of a carbonaceous residue.[52] In the 326−900 °C region, we notice a minor weight loss for *Posidonia* fibers compared to alfa and hemp due to their relatively high lignin content. Lower temperature peaks at 327.4, 328.4, and 330.5 °C, attributed to the decomposition of hemicelluloses[53] for alfa fibers, *Posidonia*, and hemp, respectively, were noted in the DTG curves. In agreement with other reported studies,[54,55] a higher residual weight at 900 °C was observed for *Posidonia* (33.9%), compared to alfa (24.1%) and hemp (22.3%), due to its higher lignin content. The results of ash content obtained by thermal decomposition performed under an air atmosphere for the last 30 min of the TGA analysis are comparable to those obtained by combustion at 600 °C. According to the calorimetric analysis, the heat of combustion (ΔH) of *Posidonia* is −18.6 kJ/g, slightly higher in absolute value than that of hemp with −17.3 kJ/g and alfa with −16.9 kJ/g, despite the higher ash content of *Posidonia*. However, these differences are low, and the values reported here, around −17 to −18 kJ/g, are typical of most lignocellulosic materials, such as wood.

Table 6. Thermal Analysis Data of *Posidonia*, Alfa, and Hemp Fibers[a,b,c,d]

sample	T_1 (°C)	T_{peak} (°C)	ash content (%)	$W_{residue}$ (%) at 900 °C	ΔH (kJ/g)
Posidonia	232.68	328.42	9.5	33.9	−18.6
Hemp	202.02	330.46	3.5	22.3	−17.3
Alfa	210.25	327.38	6.0	24.1	−16.9

[a]T_1: Initial decomposition temperature using TGA results. [b]T_{peak}: Peak temperature of DTG. [c]$W_{residue}$: TGA char residue at 900 °C. [d]ΔH: Enthalpy of combustion.

Thermal Conductivity. Figure 9 compares the thermal conductivity of *Posidonia*, alfa, and hemp airlaid panels for four densities. As expected, increasing the density led to a higher thermal conductivity due to the increase of heat transfer by conduction. Since the thermal conductivity of air within the voids is much lower than that of a solid substance, increasing the density leads to an increase of the thermal conductivity. These variations are estimated at 10% for *Posidonia* and hemp and at 9% for alfa panels when the density is increased from 40 to 90 kg/m^3. Furthermore, it can be noticed that *Posidonia* panels have the lowest thermal conductivity values for all densities. As the total open porosity of the panels was in the same range for these fibrous panels, the difference in thermal conductivity can be attributed to the intrinsic porosity of each fiber as well as the fiber arrangement into the panel. Indeed, the higher porosity of *Posidonia* fibers (76.6%) compared to alfa (57.3%) and hemp (74.8%) leads to limiting the thermal conduction component of the heat transfer. In addition, the median pore diameter of *Posidonia* (0.54 μm) was lower than those of hemp (0.61 μm) and alfa (2.1 μm) fibers. At similar porosity values, the smaller the pore size, the more the number of pores, and the path of heat transfer is increased, resulting in the reduction of heat transfer efficiency.[56] Chen et al. showed that the thermal conductivity of AAC increases by 23% when

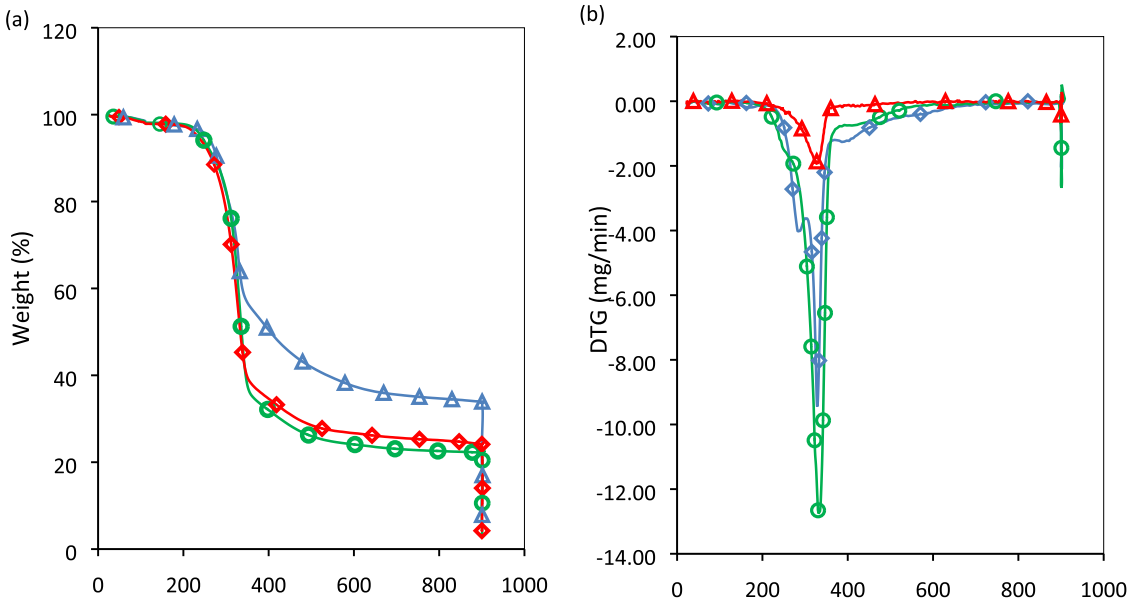

Figure 8. (a) TGA and (b) DTGA pyrolysis curves as a function of degradation temperature (°C) of *Posidonia*, Alfa, and Hemp samples. (blue straight line with triangle) Posidonia, (red straight line with diamond) Alfa, (green straight line with circle) Hemp.

https://doi.org/10.1021/acsomega.3c02481
ACS Omega 2023, 8, 48673−48688

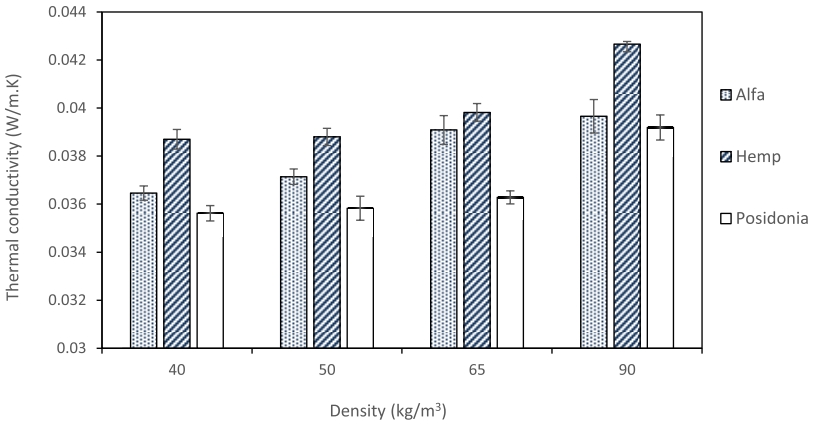

Figure 9. Thermal conductivity of *P. oceanica*, Alfa, and Hemp panels at different densities.

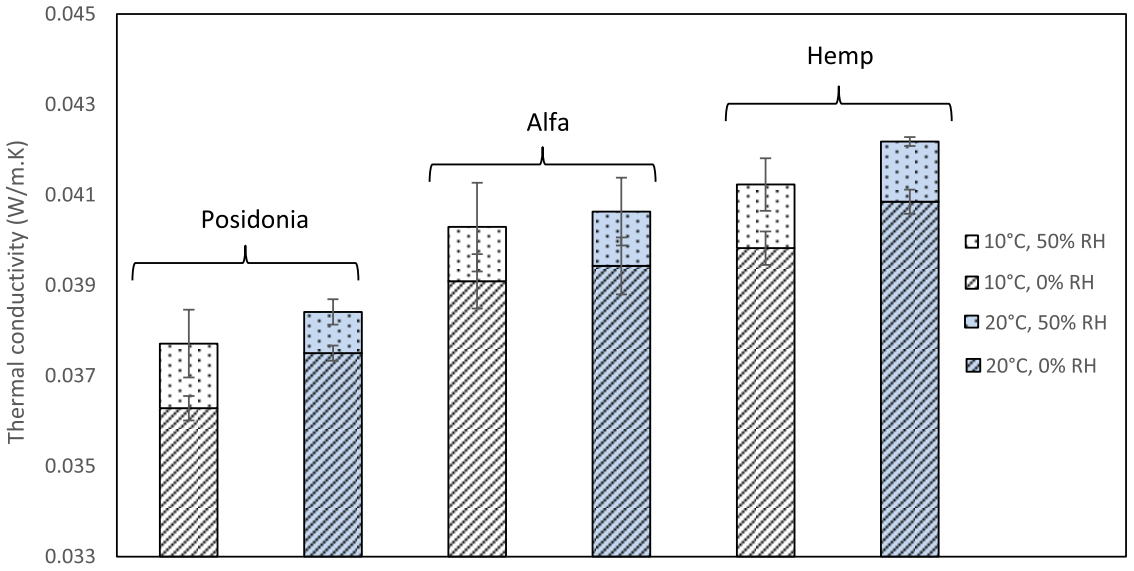

Figure 10. Thermal conductivity of *Posidonia*, Alfa, and Hemp panels at different thermal and humidity conditions.

increasing the pore size from 0.35 to 0.45 mm.[57] Even though hemp fibers have a higher porosity measured by MIP than alfa, this property was not significant enough to induce a lower thermal conductivity of hemp (0.0387−0.0427 W/(m K)) compared to alfa panels (0.0365−0.0397 W/m.K). This can be due to the high intraporosity observed on the longitudinal section of the alfa fiber (Figure 4D), which may have remained inaccessible by the mercury intrusion. Moreover, SEM images of the alfa web (Figure 7) showed a larger amount of tortuous path, creating a higher probability of elastic collisions between fibers and air and thus a lower transfer of thermal energy. In addition, the higher in-plane porosity of the alfa web (22%) allows for a smaller number of contiguous fibers, which is likely to reduce thermal conduction through the fibers compared to hemp (16%). Simultaneously, the higher content of air encapsulated in the fibrous structure of the alfa web in the plane reduces the convective component of heat, resulting in lower thermal conductivity of the alfa panels. Differences in chemical composition between fibers can also impact the thermal behaviors of panels. Hemp panels showed about 39% more cellulose than *Posidonia* and up to 32% compared to alfa. Panels based on hemp fibers, rich in cellulose, are naturally hygroscopic.[58] The hygroscopicity of cellulose content contributes to a higher moisture gain, which could occur during the thermal conductivity measurement using the flowmeter method, which took about 2 h in the dry state and up to 4 h for humid materials (50% RH). While increasing the moisture content, the thermal conductivity increases, caused mainly by conduction heat transfer of water particles[59] of the hemp sample. Besides, *Posidonia* fibers, which showed around 3 times higher lignin content (31.5%) compared to alfa (10.7%) and hemp (10.6%), had the lowest thermal conductivity values. This observation is consistent with previous studies that have shown a correlation between the lignin content and thermal conductivity. Indeed, higher lignin content results in a reduced mean free path of gas molecules, permitting a lower heat transfer of the gas phase, which contributes to a lower overall thermal conductivity of the fiber.[60,61] Wang et al.[62] also studied the thermal conductivity of lignin-PU films, with the lignin content varying from 10 to 50 wt %. They showed that from 0 to 20 wt % lignin content, the thermal conductivity was almost the same, but it decreased significantly from 20 to 50 wt % lignin. Haridevan et al.[60] showed that the incorporation of lignin into rigid polyurethane foam considerably decreased its thermal conductivity (32−34%), while Ahmad Saffian et al.[63] found that the addition of lignin to PP (30/70 wt %) only slightly increased the thermal conductivity of the resultant composite material.

https://doi.org/10.1021/acsomega.3c02481
ACS Omega 2023, 8, 48673−48688

Thermal conductivity measurements of the three panels preconditioned at 70 °C were studied for densities of 65 kg/m^3, at mean temperatures of 10 and 20 °C. The results showed that the thermal conductivity was lower at 10 °C (Figure 10). The variations were estimated to be 3.3% for seagrass, 0.8% for esparto, and 2.6% for hemp. A higher operating temperature is usually associated with a higher thermal conductivity. On increasing the temperature, the rate of heat conduction increases. On the other hand, the insulating medium (air in this case) becomes more excited, which enhances the convection within and between the voids.[64] The same trend was observed on panels preconditioned under humid conditions at 23 °C and 50% RH, and the variations were estimated at 1.8% for *Posidonia*, 0.8% for alfa, and 2.3% for hemp panels for temperatures varying from 10 to 20 °C. Thus, the temperature represents a determining factor for the thermal performance of insulating materials. The higher the temperature, the less insulating the material. This behavior could significantly impact the thermal conductivity for the winter period (internal and external building temperatures of 20 and 0 °C, respectively) and the summer period (internal and external building temperatures of 10 and 30 °C, respectively). Moreover, the comparison of the dry and wet thermal conductivity revealed the influence of moisture content on the thermal performance of these porous materials. The results showed that the thermal conductivity of wet panels (23 °C and 50% RH) increased by 3.9% for *Posidonia*, 3.1% for alfa, and 3.5% for hemp panels, compared to those obtained on dried panels at 70 °C. While increasing the moisture content, the heat conduction increases due to the presence of water particles in the sample, which engenders an increase in the thermophysical characteristics of the material.[65] It should be noted, however, that the increase in thermal conductivity under 50% relative humidity has allowed the materials to remain within the standards of thermal insulation with a thermal conductivity of <0.25 W/m.K.[66]

Table 7 compares the measured thermal conductivity of the present panels to published data for conventional thermal insulation materials. It can be noticed that the prepared airlaid panels have densities that can be included in the range of traditional insulating materials for construction, such as mineral wools, but can also be compared with agrofiber boards such as wood, kenaf, cork, and cotton fiberboards. In terms of thermal conductivity, *Posidonia*, and alfa panels are in the same range as mineral wool and can be favorably compared to most commercial products except for polyurethane foams and extruded polystyrene (XPS), which have lower thermal conductivities. Regarding the synthetic binder fibers, the developed panels contained a proportion of 10 wt % PE/PET core bicomponent fibers, comparable to that of rockwool (9 wt % PE) as well as commercialized wood fiberboards (Isonat Flex 40).

Table 7. Comparison of the Thermal Conductivity of Prepared Panels with Conventional Thermal Insulation Materials

insulation material	density (kg/m^3)	thermal conductivity (W/m.K)	reference
P. oceanica	40−90	0.0356−0.0392	present study
Alfa	40−90	0.0365−0.0397	present study
Hemp	40−90	0.0387−0.0427	present study
cork binderless boards	100−220	0.045−0.08	[67]
kenaf binderless boards	150−200	0.051−0.058	[68]
binderless cotton fiberboard	150−450	0.059−0.082	[69]
wood (pine, lauan)	450−630	0.151	[70]
polyester board	85.3−225.8	0.044−0.05	[71]
90% glass wool/9% PE	65	0.036	[72]
extruded polystyrene XPS	24−42	0.026−0.035	[73]
polyurethane foam	30−100	0.017−0.024	[74]
expanded polystyrene EPS	15−30	0.035−0.04	[67]
expanded perlite	78−224	0.0477−0.0616	[74]

This study showed that *Posidonia* fibers have a higher porosity with a finer pore diameter as well as less cellulose content than hemp fibers that are conventionally commercialized as thermal insulation materials, resulting in lower thermal conductivity.

Tensile Strength. Results of the measurement of tensile strength perpendicular to the plane of the panels are illustrated in Figure 11. The average of tensile strength is 5, 3.2, and 6.2 kPa for *Posidonia*, alfa, and hemp, respectively. Unfortunately, two out of three specimens of alfa panels got opened a few seconds ulterior to the applied load. Therefore, the results for alfa panels may not be adequately reliable. Nevertheless, from the available data, it can be seen that hemp panels had a higher tensile strength, followed by *Posidonia* panels, with a reduction of about 24%. The higher tensile strength observed on hemp panels can be attributed to its higher fiber length (46.6 ± 8.2 mm) compared to *Posidonia* (19.4 ± 13.5 mm) and alfa (41.7 ± 16.4 mm), which permits better fiber-to-fiber bonding[76] with PE/PET bicomponent fibers. Kallakas et al.[75] found a value of 0.015 MPa for hemp fiberboards with a density of 544 kg/m^3. The variability measured on each type of panel can be explained by the differences in cohesion between the natural fibers and bicomponent fibers as a result of a nonhomogeneous distribution of PE/PET fibers into the nonwoven web. In fact, some slices of alfa panels were not sufficiently consolidated, which explains their low tensile strength. However, one of the three tested alfa panels exhibited a higher value of 5.86 kPa, in the same range as that of *Posidonia* panels. This test provides an indication of fiber−fiber adhesion. Mainly, the break occurred in the slices showing a lack of bicomponent (observed during the test), suggesting that the failure process is governed by lack of fiber bonding (Figure 12). According to Pavatex data on softboards,[77] the tensile strength of wood-based softboards is 0.015 MPa. The nonwovens could be considered lightweight insulation panels and could find their use in nonstructural applications. The tensile strength perpendicular to the plane of the panels could be enhanced by improving the adhesion bond strength by ensuring a better mixture of the biobased fibers with the bicomponent fibers to permit a better interlocking into the nonwovens. Further experimental investigations are recommended toward mechanical properties to assess a better knowledge of the characteristics of the panels in comparison with current natural and synthetic thermal insulation materials.

CONCLUSIONS

The current paper presented the results of an experimental study on the use of abundant *Posidonia*, alfa, and hemp fibers to develop airlaid thermal insulation panels. These panels are

https://doi.org/10.1021/acsomega.3c02481
ACS Omega 2023, 8, 48673−48688

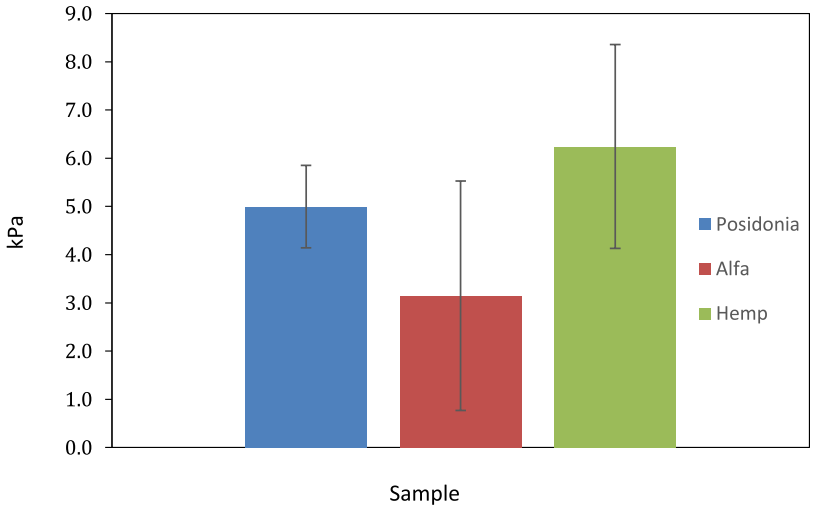

Figure 11. Tensile strength perpendicular to the plane of *Posidonia*, Alfa, and Hemp panels.

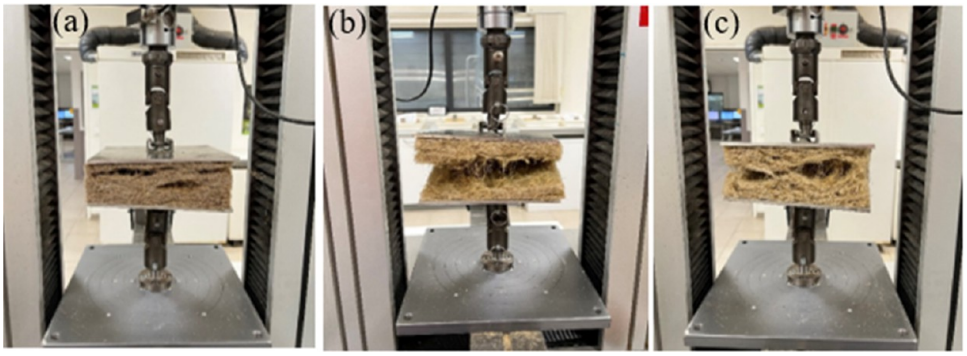

Figure 12. (a) *P. oceanica*, (b) Alfa, and (c) Hemp panels failure during the tensile strength test.

largely based on renewable resources and could find interesting applications as environmentally friendly materials, offering the possibility of replacing synthetic and mineral materials. The thermal conductivity of airlaid *Posidonia*/(PE−PET), alfa/(PE−PET), and hemp/(PE−PET) panels was found to be enhanced with the reduction of density to 40 kg/m^3 at a thickness of 40 mm. The panels presented thermal conductivity values in the same range as those of commercial mineral wool insulation products and higher than those of synthetic thermal insulation materials such as expanded polystyrene (EPS) and extruded polystyrene (XPS), but lower than those of most natural insulation products like cork, kenaf, and wood fiberboards. The physicochemical characteristics of the fibers contributed to a better understanding of the thermal behavior of the panels. The results obtained suggest several alternative uses of *Posidonia* depending on their specific features. SEM analysis showed a porous microstructure for all three fibers, which is in agreement with MIP measurements. This intrinsic porosity and the high porosity conferred by the airlaid technology (>90%) resulted in interesting thermal conductivity values of 0.0356−0.0392 W/m.K for *Posidonia* and 0.0365−0.0397 W/m.K for alfa compared to values of 0.0387−0.0427 W/m.K for hemp, for densities ranging from 40 to 90 kg/m^3, measured in the dry state. Intrusion porosimetry also validated the range of fiber density magnitude. The low density of the studied fibers compared to synthetic fibers offers the alternative of their use for lightweight insulation nonwovens or composite materials, enabling higher thermal insulation performances. Thermal analysis (TGA) revealed that the three fibers showed close thermal properties, with slightly enhanced results for *Posidonia* fibers due to their relatively higher lignin content, allowing for slower thermal decomposition. *Posidonia* panels, which showed the highest lignin content allied to the lowest cellulose content, exhibited the lowest thermal conductivity values compared to alfa and hemp, suggesting the influence of the chemical composition on the thermal performance of the natural fibers. The thermal conductivity is usually indicated as the standard value measured under dry conditions. However, ambient temperature and humidity of the environment have been found to be important parameters that affect the thermal conductivity of the airlaid panels. In future works, further mechanical properties of the airlaid panels and their recyclability will be investigated to expand their use in the thermal insulation field. We hope that this work on *Posidonia*, alfa, and hemp fibers will contribute to the development of low-cost natural thermal insulation materials for various applications such as buildings, automotive, or other industrial sectors.

■ ASSOCIATED CONTENT

Supporting Information

The Supporting Information is available free of charge on the ACS Publication Web site. The Supporting Information is available free of charge at https://pubs.acs.org/doi/10.1021/acsomega.3c02481.

https://doi.org/10.1021/acsomega.3c02481
ACS Omega 2023, 8, 48673−48688

Intrusion/extrusion curves for fibers and ground fibers as functions of pressure of *Posidonia*, hemp, and alfa from MIP measurements; schematic presentation and SEM micrographs of the different steps of alfa fiber extraction; general view of thermal insulation panels made of *P. oceanica* fibers through the airlaid process; and SEM micrographs of nonwoven panels showing bicomponent fibers interlocking points for *Posidonia*, alfa, and hemp after thermal consolidation (PDF)

AUTHOR INFORMATION

Corresponding Author

Nicolas Brosse − *LERMAB, Université de Lorraine, F54000 Nancy, France;* orcid.org/0000-0001-8505-8401; Email: nicolas.brosse@univ-lorraine.fr

Authors

Melek Ayadi − *Centre d'Essais Textile Lorrain CETELOR, F88000 Epinal, France; Laboratoire de Génie Textile, Université de Monastir, 5070 Monastir, Tunisie; LERMAB, Université de Lorraine, F54000 Nancy, France*

César Segovia − *Centre d'Essais Textile Lorrain CETELOR, F88000 Epinal, France*

Ayda Baffoun − *Textile Materials and Process Research Unit, University of Monastir, 5019 Monastir, Tunisia*

Riadh Zouari − *Laboratoire de Génie Textile, Université de Monastir, 5070 Monastir, Tunisie*

Vanessa Fierro − *Université de Lorraine, CNRS, IJL, F88000 Epinal, France;* orcid.org/0000-0001-7081-3697

Alain Celzard − *Université de Lorraine, CNRS, IJL, F88000 Epinal, France; Institut Universitaire de France (IUF), F75005 Paris, France;* orcid.org/0000-0003-0073-9545

Slah Msahli − *Laboratoire de Génie Textile, Université de Monastir, 5070 Monastir, Tunisie*

Complete contact information is available at: https://pubs.acs.org/10.1021/acsomega.3c02481

Author Contributions

M.A.: Investigation, conceptualization. A.B.: Methodology, investigation, analysis. R.Z.: Methodology, investigation, analysis. C.S.: Methodology, investigation, analysis. V.F.: Methodology, investigation, Analysis. A.C.: Methodology, investigation, analysis. S.M.: Project administration and supervision. N.B.: Project administration and supervision.

Funding

This study is part of a PHC Utique project (Isolation thermique et sonore par un nontissé écologique, Code 44228PK). The authors would also like to acknowledge the University of Monastir for the financial support.

Notes

The authors declare no competing financial interest.

ACKNOWLEDGMENTS

The authors would like to thank Philippe Gadonneix (Université de Lorraine, IJL) for the measurements using AutoTap, Geopyc, Accupyc, and Autopore devices. The authors would also like to thank Mohamed Ragoubi (UniLaSalle) for chemical analysis using the Foss device. The authors acknowledge the Roberval Laboratory and the UTC (Université de Technology de Compiègne) where porosity measurements on panels were processed.

ABBREVIATIONS

EDS, energy-dispersive spectroscopy; SEM, scanning electron microscopy; XRF, X-ray fluorescence; PE, polyethylene terephthalate; PET, polyester

REFERENCES

(1) EU Commission-CORDIS. Final Report Suammary-ECOLAS-TANE-A Novel Technology for Producing Biobased Synthetic Textile Fibers from Biomass-derived furanic monomers. https://cordis.europa.eu/project/id/298619/reporting.

(2) *Global Carbon Project. Supplemental data of Global Carbon Budget (Version 1.0)* 2021.

(3) IEA. *Global Energy Review: CO_2 Emissions in 2020*; IEA: Paris, 2021.

(4) Sandin, G.; Roos, S.; Johansson, M.*Environmental Impact of Textile Fibers−What We Know and What We Don't Know: Fiber Bible Part 2*, 2019.

(5) Arpitha, G. R.; Sanjay, M. R.; Senthamaraikannan, P.; Barile, C.; Yogesha, B. Hybridization Effect of Sisal/Glass/Epoxy/Filler Based Woven Fabric Reinforced Composites. *Exp. Tech.* **2017**, *41*, 577−584, DOI: 10.1007/s40799-017-0203-4.

(6) Akin, D. E. Chemistry of Plant Fibres. In *Industrial Applications of Natural Fibres: Structure, Properties and Technical Applications-Part 1*; Müssig, J., Ed.; 2010; pp 13−22 DOI: 10.1002/9780470660324.

(7) Santhosh Kumar, S.; Hiremath, S. S.Natural Fiber Reinforced Composites in the Context of Biodegradability: A Review. In *Encyclopedia of Renewable and Sustainable Materials* 2020; Vol. *5*, pp 160−178 DOI: 10.1016/B978-0-12-803581-8.11418-3.

(8) Davies, P.; Morvan, C.; Sire, O.; Bale, C. Structure and properties of fibres from sea-grass (*Zostera marina*). *J. Mater. Sci.* **2007**, *42* (13), 4850−4857.

(9) Khiari, R.; Marrakchi, Z.; Belgacem, M. N.; Mauret, E.; Mhenni, F. New lignocellulosic fibres-reinforced composite materials: A stepforward in the valorisation of the *Posidonia oceanica* balls. *Compos. Sci. Technol.* **2011**, *71* (16), 1867−1872.

(10) Green, E. P.; Short, F. T.; UNEP-WCMC. *World Atlas of Seagrasses: Present Status and Future Conservation*; University of California Press: Berkeley and Los Angeles, 2003 0−520−24047−2.

(11) Lefebvre, L.; Compère, P.; Léonard, A.; Plougonven, E.; Vandewalle, N.; Gobert, S. Mediterranean aegagropiles from *Posidonia oceanica* (L.) Delile (1813): a first complete description from macroscopic to microscopic structure. *Mar. Biol.* **2021**, *168* (3), No. 37.

(12) LFG Energy Project Development Handbook, Landfill Methan Outreach Program 2021 https://www.epa.gov/system/files/documents/2021-07/pdh_full.pdf.

(13) Maciá, A.; Baeza, F. J.; Saval, J. M.; Ivora, S. Mechanical properties of boards made in biocomposites reinforced with wood and *Posidonia Oceanica* fibers. *Composites, Part B* **2016**, *104*, 1−8.

(14) Carmona, C.; Horrach, G.; Olivier, C.; Forteza, F. J.; Munoz, J. *Posidonia oceanica* como aislamiento térmico: Determinación de la densidad aparente mínima, según requisitos de proyecto, para su utilización como solución constructiva en cubierta plana. *Rev. Constr.* **2018**, *17*, 250−257.

(15) Beroual, M.; Boumaza, L.; Mehelli, O.; Trache, D.; Tarchoun, A. F.; Khimeche, K. Physicochemical properties and thermal stability of microcrystalline cellulose isolated from esparto grass using different delignification approaches. *J. Polym. Environ.* **2021**, *29*, 130−142.

(16) Marion, J. L'alfa, matière première pour l'industrie pametière. *Rev. For. Fr.* **1958**, *7*, 345−347.

(17) Célérier, J.; Cholley, A. La production de l'alfa en Afrique du Nord. *Annales de géographie* **1931**, *225*, 323−325.

(18) Elhamdouni, Y.; Khabbazi, A.; Benayad, C.; Dadi, A.; Ahmid, O. I. Effect of fiber alfa on thermophysical characteristics of a material based on clay. *Energy Procedia* **2015**, *74*, 718−727.

(19) Ajouguim, S.; Djelal, C.; Page, J.; Waqif, M.; Abdelouahdi, K.; Saâdi, L. Experimental investigation on the use of alfa fibers as

reinforcement of cimentitious materials. *Acad. J. Civ. Eng.* **2019**, *37* (2), 557−563.
(20) El-Abbassi, F. E.; Assarar, M.; Ayad, R.; Lamdouar, N. Effect of alkali treatment on Alfa fibre as reinforcement for polypropylene based eco-composites: mechanical behaviour and water ageing. *Compos. Struct.* **2015**, *133*, 451−457.
(21) Arrakhiz, F.; Elachaby, M.; Bouhfid, R.; Vaudreuil, S.; Essassi, M.; Qaiss, A. Mechanical and thermal properties of polypropylene reinforced with Alfa fiber under different chemical treatment. *Mater. Des.* **2012**, *35*, 318−322.
(22) Hanana, S.; Elloumi, A.; Placet, V.; Tounsi, H.; Belghith, H.; Bradai, C. An efficient enzymatic-based process for the extraction of high-mechanical properties alfa fibres. *Ind. Crops Prod.* **2015**, *70*, 190−200.
(23) FAOSTAT. Textile Exchange 2020 https://www.fao.org/faostat/en/#data/FO%20. (accessed%202021−10−05).
(24) Väisänen, T.; Kilpeläinen, P.; Kitunen, V.; Lappalainen, R.; Tomppo, L. Effect of steam treatment on the chemical composition of hemp (*Cannabis sativa* L.) and identification of the extracted carbohydrates and other compounds. *Ind. Crops Prod.* **2019**, *131*, 224−233.
(25) INDA and EDANA Release. *European Non-Woven Market Insights* 2021.
(26) Wilson, A.The Formation of Dry, Wet, Spunlaid, and Other Types of Nonwovens. In *Applications of Nonwovens in Technical Textiles*; Woodhead Publishing, 2010; pp 3−17 DOI: 10.1533/9781845699741.1.3.
(27) Van Soest, P.; Robertson, J. *Analysis of Forages and Fibrous Foods*; Department of Animal Science, Cornell University: Ithaca, USA, 1985.
(28) Célino, A.; Fréour, S.; Jacquemin, F.; Casari, P. The hygroscopic behavior of plant fibers: a review. *Front. Chem.* **2014**, *1*, No. 43.
(29) Brouwer, P. *Theory of XRF*; PaNalytical B.V.: Almelo, Netherlands, 2013. https://www.iotcco.com/uploads/VirtualTeaching/Articles/PANanalytical/PANanalytical%20XRF%20theory.pdf.
(30) Reza, S.; Chang, H.; Norlin, B.; Fröjdh, C.; Thungstrom, G.Detecting Cr Contamination in Water Using X-ray Fluorescence. In *2015 IEEE Nuclear Science Symposium and Medical Imaging Conference (NSS/MIC)*; IEEE, 2015; pp 1−2.
(31) Sun, C. C. A novel method for deriving true density of pharmaceutical solids including hydrates and water-containing powders. *J. Pharm. Sci.* **2004**, *93*, 646−653.
(32) Junghans, K.; Niemz, P.; Bächle, F. Untersuchungen zum Einfluss der thermischen Vergütung auf die Porosität von Fichtenholz. *Holz Roh- Werkst.* **2005**, *63*, 243−344.
(33) Washburn, E. W. The dynamics of capillary flow. *Phys. Rev.* **1921**, *17*, 273−283.
(34) Beranek, L. L. Acoustic Impedance of Porous Materials. *J. Acoust. Soc. Am.* **1942**, *13*, 248−260.
(35) Apostolaki, E. T.; Caviglia, L.; Santinelli, V.; Cundy, A. B.; Tramati, C. D.; Mazzola, A.; Vizzini, S. The importance of dead seagrass (*Posidonia Oceanica*) matte a biochemical sink. *Front. Mar. Sci.* **2022**, *9*, No. 861998.
(36) *Handbook of Fiber Chemistry*, 3rd ed.; Lewin, M., Ed.; International Fiber Science and Technology Series, 2007. http://library.navoiy-uni.uz/files/lewin%20m.%20(ed.)%20-%20handbook%20of%20fiber%20chemistry%20(3d%20edinion)(2007)(1044s).pdf.
(37) Ncibi, M. C.; Jeanne-Rose, V.; Mahjoub, B.; Jean-Marius, C.; Lambert, J.; Ehrhardt, J.-J.; Bercion, Y.; Seffen, M.; Gaspard, S. Preparation and characterization of raw chars and physically activated carbons derived from marine *Posidonia Oceanica* (L.) fibers. *J. Hazard. Mater.* **2009**, *165*, 240−249.
(38) Khiari, R.; Mhenni, M. F.; Belgacem, M. N.; Mauret, E. Chemical composition and pulping of date palm rachis and Posidona Oceanica − A comparison with other wood and non-wood fibre sources. *Bioresour. Technol.* **2010**, *101*, 775−780.
(39) Jiménez, L.; Rodrigues, A.; Perez, A.; Moral, A.; Serrano, L. Alternative raw materials and pulping process using clean technologies. *Ind. Crops Prod.* **2008**, *28*, 11−16.
(40) Copur, Y.; Tozluoglu, A. A comparison of kraft, PS, kraft-AQ and kraft-$NaBH_4$ pulps of Brutia pine. *Bioresour. Technol.* **2008**, *99*, 909−913.
(41) Fiserova, M.; Gigac, J.; Majtnerova, A. N.; Szeiffova, G. A. Evaluation of annual plants (*Amaranthus caudatus* L., *Atriplex hortensis* L., *Helianthus tuberosus* L.) for pulp production. *Cellul. Chem. Technol.* **2006**, *40*, 405.
(42) Tahir, P. M.; Ahmed, A. B.; SifulAzry, S. O.; Ahmed, Z. Retting Process of Some Bast Plant Fibers and Its Effect on Fiber Quality: A Review. *BioResources* **2011**, *6*, 5260−5281.
(43) Pereira, P. H.; Rosa, M. D.; Cioffi, M. O.; Benini, K. C.; Milanese, A. C.; Voorwald, H. J.; Mulinari, D. R. Vegetal Fibers in Polymeric Composites: A Review. *Polímeros* **2015**, *25*, 9−22.
(44) Bouiri, B.; Amrani, M. Production of dissolving grade pulp from Alfa. *Bioresources* **2010**, *5*, 291−302.
(45) El-Abbassi, F. E.; Assarar, M.; Ayad, R.; Bourmaud, A.; Baley, C. A review on alfa fibre (*Stipa tenacissima* L.): From the plant architecture to the reinforcement of polymer composites. *Composites, Part A* **2020**, *128*, 105677.
(46) Mehdadi, Z.; Benaouda, Z.; Latreche, A.; Benhassaini, H.; Belbraouet, S. Évolution saisonnière de la composition foliaire de *Stipa tenacissima* L. en éléments minéraux et en fibres pariétales. *Acta Bot. Gallica* **2008**, *155*, 435−445.
(47) Thomsen, A. B.; Klinke, H. B.; Schmidt, A. S. Conversion of Plant Residues to Value Added Products. In *1st World Conference on Biomass for Energy and Industry*; James & James (Science Publishers), 2001; pp 1075−1077.
(48) Akchiche, O.; Khadra, M. Esparto grass (*stipa tenacissima* l), raw material of papermaking. *First part. Chem. Plant Mater.* **2007**, *4*, 25−30.
(49) Wahab, M. A.; Hassine, R. B.; Jellali, S. Removal of phosphorus from aqueous solution by *Posidonia oceanica* fibers using continuous stirring tank reactor. *J. Hazard. Mater.* **2011**, *189*, 577−585.
(50) Ayadi, M.; Zouari, R.; Segovia, C.; Baffoun, A.; Msahli, S.; Brosse, N.Development of Airlaid Non-woven panels for building's thermal insulation. In *International Conference of Applied Research on Textile and Materials*; Springer International Publishing: Cham, 2022; pp 110−117 DOI: 10.4028/www.scientific.net.
(51) Pickering, K. L.; Efendy, M. G. A.; Le, T. M. A review of recent developments in natural fibre composites and their mechanical performance. *Composites, Part A* **2016**, *83*, 98−112.
(52) Trache, D.; Donnot, A.; Khimeche, K.; Benelmir, R.; Brosse, N. Physico-chemical properties and thermal stability of microcrystalline cellulose isolated from Alfa fibres. *Carbohydr. Polym.* **2014**, *104*, 223−230.
(53) Le Troedec, M.; Sedan, D.; Peyratout, C.; Bonnet, J. P.; Smith, A.; Guinebretiere, R.; Gloaguen, V.; Krausz, P. Influence of various chemical treatments on the composition and structure of hemp fibres. *Composites, Part A* **2008**, *39*, 514−522.
(54) Tarchoun, A. F.; Trache, D.; Klapötke, T. M. Microcrystalline cellulose from *Posidonia oceanica* brown algae: Extraction and characterization. *Int. J. Biol. Macromol.* **2019**, *138*, 837−845.
(55) Abdul Khalil, H. P.; Lai, T. K.; Tye, Y. Y.; Paridah, M. T.; Fazita, M. N.; Azniwati, A. A.; Dungani, R.; Rizal, S. Preparation and Characterization of Microcrystalline Cellulose from Sacred Bali Bamboo as Reinforcing Filler in Seaweed-based Composite Film. *Fibers. Polym.* **2018**, *19*, 423−434.
(56) Jin, H. Q.; Yao, X. L.; Fan, L. W.; Xu, X.; Yu, Z. T. Experimental determination and fractal modeling of the effective thermal conductivity of autoclaved aerated concrete: Effects of moisture content. *Int. J. Heat Mass Transfer* **2016**, *92*, 589−602.
(57) Chen, G.; Li, F.; Jing, P.; Geng, J.; Si, Z. Effect of Pore Structure on Thermal Conductivity and Mechanical Properties of Autoclaved Aerated Concrete. *Materials* **2021**, *14* (2), 339.

https://doi.org/10.1021/acsomega.3c02481
ACS Omega 2023, 8, 48673−48688

(58) Tye, R. P.; Spinney, S. C. A study of the effects of moiture vapour on the thermal transmittance characteristics of cellulose fibre thermal insulation. *J. Therm. Insul.* **1979**, *2*, 175−196.
(59) Zhou, J.; Zhou, H.; Hu, C.; Hu, S. Measurement of thermal and dielectric properties of medium density fiberboard with different moisture contents. *BioResources* **2013**, *8* (3), 4185−4192.
(60) Haridevan, H.; McLaggan, M. S.; Evans, D. A.; Martin, D. J.; Seaby, T.; Zhang, Z.; Annamalai, P. Dispersion Methodology for Technical Lignin into Polyester Polyol for High-Performance Polyurethane Insulation Foam. *ACS Appl. Polym. Mater.* **2021**, *3*, 3528−3537.
(61) Pan, X.; Saddler, J. N. Effect of Replacing Polyol by Organosolv and Kraft Lignin on the Property and Structure of Rigid Polyurethane Foam. *Biotechnol. Biofuels* **2013**, *6*, 12.
(62) Wang, Z.; Yang, X.; Zhou, Y.; Liu, C. Mechanical and Thermal Properties of Polyurethane Films from Peroxy-acid Wheat Straw Lignin. *BioResources* **2013**, *8* (3), 3833−3843.
(63) Ahmad Saffian, H.; Talib, M. A.; Lee, S. H.; Md Tahir, P.; Lee, C. H.; Ariffin, H.; Asa'ari, A. M. Mechanical Strength, Thermal Conductivity and Electrical Breakdown of Kenaf Core Fiber/Lignin/Polypropylene Biocomposite. *Polymers* **2020**, *12*, 1833.
(64) Willoughby, J.Insulation. In *Plant Engineer's Reference Book*; Butterworth-Heinemann, 2002; pp 30−1−30−18 DOI: 10.1016/b978-075064452-5/50085-7.
(65) Modi, S. K.; Durga Prasad, B.; Basavaraj, M. Effect of moisture content and temperature on thermal conductivity of *Psidium guajava* L. by line heat source method (transient analysis). *Int. J. Heat Mass Transfer* **2014**, *78*, 354−359.
(66) Karwa, R. One-Dimensional Steady State Heat Conduction. In *Heat Mass Transfer*; Karwa, R., Ed.; Springer: Singapore, 2017; pp 7−116 .
(67) Margit, P.; Roland, G.; Martins, H. S.; Alexander, R. Insulating Materials; Principle, Materials, Application *First Edition, electronic version* 2008.
(68) Suleiman, B. M.; Larfeldt, J.; Leckner, B.; Gustavsson, M. Thermal conductivity and diffusivity of wood. *Wood Sci. Technol.* **1999**, *33*, 465−473.
(69) Zhou, X. Y.; Zheng, F.; Li, H. G.; Lu, C. L. An environment-friendly thermal insulation material from cotton stalk fibers. *Energy Build.* **2010**, *42* (7), 1070−1074.
(70) Xu, J.; Sugawara, R.; Widyorini, R.; Han, G. P.; Kawai, S. Manufacture and properties of low-density binderless particleboard from kenaf core. *J. Wood Sci.* **2004**, *50*, 62−67.
(71) Antolinc, D.; Filipič, K. E. Recycling of Nonwoven Polyethylene Terephthalate Textile into Thermal and Acoustic Insulation for More Sustainable Buildings. *Polymers* **2021**, *13* (18), 3090.
(72) Klamer, M.; Morsing, E.; Husemoen, T. Fungal growth on different insulation materials exposed to different moisture regimes. *Int. Biodeterior. Biodegrad.* **2004**, *54* (4), 277−282.
(73) Segovia, F.; Blanchet, P.; Auclair, N.; Essoua Essoua, G. G. Thermo-mechanical properties of a wood fiber insulation. *Buildings* **2020**, *10* (9), 152.
(74) ASTM Standard C 168−97 *Terminology Relating to Thermal Insulating Material* 1997.
(75) Kallakas, H.; Närep, M.; Närep, A.; Poltimäe, T.; Kers, J. Mechanical and physical properties of industrial hemp-based insulation materials. *Proc. Est. Acad. Sci.* **2018**, *67* (2), 183−192.
(76) Larsson, P. T.; Lindström, T.; Carlsson, L. A.; Fellers, C. Fiber length and bonding effects on tensile strength and toughness of kraft paper. *J. Mater. Sci.* **2018**, *53* (3), 3006−3015.
(77) Acara Concepts. http://www.acaracocepts.com/wp-content/themes/acaraconcepts/pdfs/Brochure-Pavatex-Products&Application.pdf. (accessed 2018−03−29).

https://doi.org/10.1021/acsomega.3c02481
ACS Omega 2023, 8, 48673−48688